JOURNAL OF PROPULSION AND POWER
Vol. 14, No. 2, March–April 1998

Blading Response to Potential Field Interactions in Axial- and Radial-Flow Turbomachinery

Albert J. Sanders* and Sanford Fleeter†
Purdue University, West Lafayette, Indiana 47907

An unsteady aerodynamic model is developed to predict the response of both axial- and radial-flow turbomachinery blading resulting from potential field interactions. For axial-flow turbomachines this is accomplished by extending a compressible flat-plate cascade analysis to account for the induced velocities due to an adjacent blade row's potential field. The blading response in a radial cascade consisting of logarithmic spiral airfoils is then calculated utilizing a conformal transformation mapping of the radial geometry to an equivalent axial cascade, enabling existing axial cascade models to be used for radial-flow turbomachine blade rows. This model is then used to demonstrate the forced response characteristics of a blade row to potential fields of both upstream and downstream airfoil rows and to upstream blade-row-generated vortical wakes, including the differences between the response of axial- and radial-flow turbomachinery blading. For both the axial- and radial-flow blade rows, the nondimensional unsteady aerodynamic response amplitudes generated by airfoil row potential and vortical wake-forcing functions were of the same order of magnitude. Thus, for closely spaced, highly loaded blade rows, both wake and potential field interactions may be of equal significance.

Nomenclature

a = speed of sound
C = airfoil chord
C_L = unsteady lift coefficient
C_M = unsteady moment coefficient
$C_{\Delta p}$ = unsteady pressure difference coefficient
k = reduced frequency based on chord
k_ξ, k_η = axial and tangential wave numbers
M = Mach number
N, N_{exc} = number of airfoils in responding and excitation-producing airfoil rows
p = static pressure perturbation
R = diffuser inlet to impeller exit radius ratio
r, θ = radial and circumferential coordinates
r_0 = radial cascade exit radius
S, S_{exc} = tangential spacing of responding and excitation-producing airfoil rows
t = time
U, V = axial and tangential velocities
U_w = rotor wheel speed
u, v = axial and tangential velocity perturbations
W = streamwise velocity
w = upwash velocity
X, Y = chordwise and transverse coordinates
α_L = radial cascade logarithmic spiral angle, positive ccw
γ = bound vorticity, positive ccw
$\Delta\bar{p}$ = unsteady pressure difference, upper–lower
Δr = airfoil radial extent in radial cascade
$\Delta\eta$ = phase shifting constant
$\Delta\xi$ = axial spacing between airfoil rows
ε = free vorticity in wake, positive ccw
Θ = stagger angle, positive ccw
ξ, η = axial and tangential coordinates
ρ = density
σ = interblade phase angle
Φ = perturbation velocity potential
ϕ = flow coefficient based on cascade inlet conditions
χ = compressibility factor
ω = excitation frequency, rad/s

Subscripts

A, R = quantities associated with axial and radial cascades
r, θ = radial and circumferential components
up, dn = perturbations due to upstream and downstream airfoil row potential fields
w = perturbation due to upstream vortical wake
ξ, η = axial and tangential components
$+$, $-$ = upper and lower airfoil surfaces
∞ = freestream value

Superscript

$-$ = complex amplitude

Introduction

MODERN turbomachines are often plagued by flow-induced forced vibration problems resulting from unsteady aerodynamic interactions between adjacent blade rows. These interactions are a result of the blading passing through spatially periodic flow nonuniformities generated by the potential flowfields of both upstream and downstream airfoil rows and of the viscous wakes created by upstream airfoils. The potential field is a steady circumferentially nonuniform disturbance that results from the thickness and lifting properties of the blading. This type of disturbance decays exponentially with distance, usually with a characteristic length equal to the tangential spacing of the blade row. Viscous wakes are total pressure deficits that result from the boundary layers on upstream airfoils. These vortical disturbances convect with the mean flow and decay very slowly with distance, usually persisting for several airfoil chord lengths.

The design trends of both axial- and radial-flow turbomachines have resulted in these blade row interactions becoming increasingly significant. Axial-flow compressors and turbines are being designed with closely spaced, highly loaded blade

Received April 15, 1997; revision received Oct. 15, 1997; accepted for publication Oct. 24, 1997.

*Research Assistant, School of Mechanical Engineering, 1003 Chaffee Hall. Student Member AIAA.

†McAllister Distinguished Professor, School of Mechanical Engineering, 1003 Chaffee Hall. Associate Fellow AIAA.

rows, resulting in increased unsteady aerodynamic interactions. Dring et al.[1] experimentally investigated the interaction between an axial-flow turbine nozzle and rotor for axial spacings of 15 and 65% of the nominal axial chord. With the 15% gap, the potential field of the downstream rotor had a considerable influence on the upstream nozzle row, with the pressure fluctuations as high as 15% of the dynamic pressure at the stage exit. The fluctuating pressure at the leading edge of the downstream rotor was also found to be as high as 80% of the inlet dynamic pressure. When the axial gap was increased, the fluctuating pressure on the rotor decreased, typically by a factor of 2. The performance of the turbomachine is also influenced by the spacing between the adjacent blade rows, with decreased axial spacing resulting in increased efficiency and pressure rise of a low-speed research compressor.[2]

There are analogous results in radial-flow turbomachines. Namely, in centrifugal compressors, vaned or channel diffusers are utilized because they are more compact and have a higher pressure recovery than vaneless configurations of the same size. This results in a significant improvement in both the efficiency and pressure rise capabilities of the stage. Arndt et al.[3] experimentally investigated the diffuser vane response caused by blade row interactions in a high-performance turbopump, with radial spacings ranging from 1.5 to 4.5% of the impeller exit radius. The amplitude of the ensemble-averaged lift was up to three times as large as the steady lift for a radial spacing of 1.5% and twice as large for a radial spacing of 4.5%. Also analyzed were both the impeller blade and the diffuser vane responses for several vaned diffuser configurations with radial spacings ranging from 5 to 8% of the impeller exit radius. For small radial spacings, the pressure fluctuations on both the impeller blades and diffuser vanes were up to the same order of magnitude as the total pressure rise across the pump.[4]

The analyses widely used by gas turbine manufacturers to predict unsteady aerodynamic forces are largely based on classical linear theory developed for axial-flow turbomachines. Kemp and Sears[5] were the first to calculate the blading response caused by potential flow interactions. Whitehead[6] and Smith[7] incorporated the effects of adjacent airfoils and compressibility, which greatly extended the application of classical linearized airfoil theory to cascade representations of turbomachine blade rows. Advanced analyses have been developed that model thickness and camber in the responding blade row, thereby distorting the perturbation by linearizing about the nonuniform steady flow around the airfoil rather than the simpler upstream uniform flow.[8–10] A forced response prediction system to analyze the rotor blade response to its interaction with the potential field of a downstream vane–strut configuration was developed by Chiang and Turner.[11] The steady-state static pressure perturbation upstream of the vane–strut configuration was determined at the location of the rotor exit plane using an implicit two-dimensional computational fluid dynamics (CFD) solver. This static pressure perturbation was then assumed to be at the rotor inlet and transformed to the rotating blade coordinate system. In their unsteady aerodynamic analysis it was assumed that the velocity perturbation due to this static pressure field was simply convected with the mean flow past the responding airfoils.

In contrast to the extensive literature on axial-flow blade rows, relatively little attention has been focused on modeling blade row interactions in radial-flow turbomachines. Simpson et al.[12] developed a model to predict the hydraulic noise generated by the unsteady impeller–diffuser–volute interaction in a centrifugal pump based on conformal mapping to relate the fluctuating pressure as determined from a generalization of the Kemp and Sears analysis[5] to a radial-flow stage consisting of logarithmic spiral airfoils. Bryan and Fleeter[13] developed a model to predict the radial cascade blading response due to pitching and plunging airfoil motions, as well as a convected vortical gust based on mapping a solution obtained from the flat-plate cascade model of Smith[7] to a radial cascade of logarithmic spiral airfoils.

In summary, closely spaced blade rows of both axial- and radial-flow turbomachines can result in improved performance and efficiency while reducing the machine's size and weight. However, these closely spaced blade rows can lead to unacceptable vibratory stress levels. As a result, first-principle design systems must be developed that can accurately predict the blading response for closely spaced blade rows, i.e., in addition to vortical gusts, the influence of the potential fields of the adjacent blade rows must be analyzed. This paper addresses this need, developing a first-order linear prediction of the blading response due to potential field interactions in both axial- and radial-flow turbomachines. For axial-flow turbomachines, this is accomplished by extending the compressible flat-plate cascade analysis of Smith[7] to include the upwash velocities induced by the potential fields of adjacent airfoil rows. The blading response in a radial cascade consisting of logarithmic spiral airfoils is then calculated utilizing a conformal transformation mapping of the radial-flow geometry to an equivalent axial cascade, thereby enabling existing axial cascade models to be used for radial-flow turbomachine blade rows.

Axial Cascade Unsteady Analysis

The linear theory model to predict the unsteady loading on an axial-flow blade row due to its unsteady interaction with an adjacent airfoil row considers a two-dimensional flat-plate cascade in a subsonic inviscid isentropic uniform flow field (Fig. 1). The unsteady flow is assumed to be a small perturbation to the uniform mean flow, leading to the following linearized continuity and momentum equations:

$$\frac{\partial p}{\partial t} + U_\infty \frac{\partial p}{\partial \xi} + V_\infty \frac{\partial p}{\partial \eta} + \rho_\infty a_\infty^2 \left(\frac{\partial u}{\partial \xi} + \frac{\partial v}{\partial \eta} \right) = 0 \tag{1}$$

$$\frac{\partial u}{\partial t} + U_\infty \frac{\partial u}{\partial \xi} + V_\infty \frac{\partial u}{\partial \eta} + \frac{1}{\rho_\infty} \frac{\partial p}{\partial \xi} = 0 \tag{2a}$$

$$\frac{\partial v}{\partial t} + U_\infty \frac{\partial v}{\partial \xi} + V_\infty \frac{\partial v}{\partial \eta} + \frac{1}{\rho_\infty} \frac{\partial p}{\partial \eta} = 0 \tag{2b}$$

where the speed-of-sound equation for the isentropic flow of a calorically perfect gas has been substituted into the continuity equation.

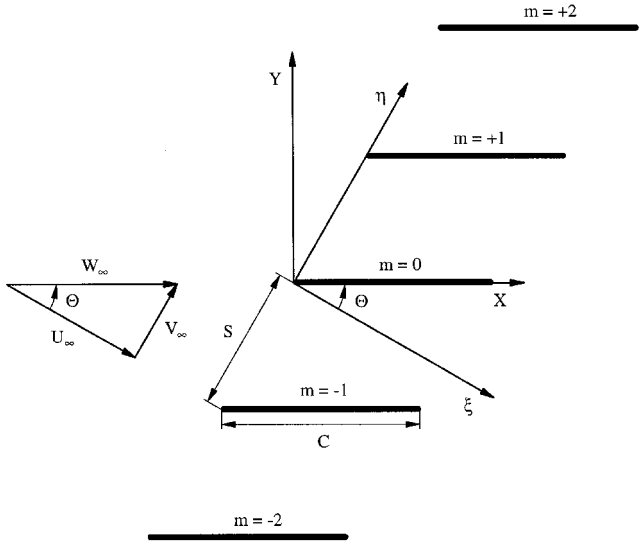

Fig. 1 Flat-plate cascade geometry.

The unsteady flow is assumed to be harmonic in space and time

$$p = \bar{p} \exp[i(k_\xi \xi + k_\eta \eta + \omega t)] \tag{3a}$$

$$u = \bar{u} \exp[i(k_\xi \xi + k_\eta \eta + \omega t)] \tag{3b}$$

$$v = \bar{v} \exp[i(k_\xi \xi + k_\eta \eta + \omega t)] \tag{3c}$$

where the complex constants $\bar{p}$, $\bar{u}$, and $\bar{v}$, the axial and tangential wave numbers k_ξ and k_η, and the frequency ω are to be determined.

Substituting these harmonic solutions into the linearized continuity and momentum equations results in the following characteristic equation that has two families of solutions:

$$(\omega + U_\infty k_\xi + V_\infty k_\eta)[(\omega + U_\infty k_\xi + V_\infty k_\eta)^2 - a_\infty^2(k_\xi^2 + k_\eta^2)] = 0 \tag{4}$$

With $(\omega + U_\infty k_\xi + V_\infty k_\eta) = 0$, the solution corresponds to a vorticity wave that is simply convected with the mean flow with no associated static pressure fluctuation. The axial wave number for this type of disturbance is

$$k_\xi = -\frac{(\omega/a_\infty + k_\eta M \sin \Theta)}{M \cos \Theta} \tag{5}$$

If $(\omega + U_\infty k_\xi + V_\infty k_\eta)^2 - a_\infty^2(k_\xi^2 + k_\eta^2) = 0$, the solution corresponds to a pair of irrotational pressure waves, one propagating upstream and the other downstream at the speed of sound. The axial wave numbers for these pressure waves are

$$k_\xi = \left[M \cos \Theta(\omega/a_\infty + k_\eta M \sin \Theta) \pm \sqrt{(\omega/a_\infty + k_\eta M \sin \Theta)^2 - (1 - M^2 \cos^2\Theta)k_\eta^2}\right] / (1 - M^2 \cos^2\Theta) \tag{6}$$

When the argument under the radical is positive, the axial wave number is real and the waves propagate away from the cascade unattenuated. If the argument is negative, the waves decay exponentially. With the argument zero, only one wave is created, propagating in the tangential direction. This is an acoustic resonance condition often referred to as the cut-on or cutoff point.

The tangential wave number is determined from unsteady periodicity requirements

$$k_\eta = (\sigma - 2\pi r)/S \qquad r = 0, \pm 1, \pm 2, \ldots \tag{7}$$

where σ specifies the time or phase lag between unsteady flow phenomena acting on adjacent airfoils. Note that σ is a function of the number of unsteady disturbances around the annulus and the number of airfoils in the responding blade row, specifically $\sigma = \pm 2\pi(N_{\text{exc}}/N) = \pm 2\pi(S/S_{\text{exc}})$, with N_{exc} the number of incident disturbances of tangential wavelength S_{exc}, and N the number of airfoils in the responding blade row with tangential spacing S, with the plus sign used if the responding blade row of interest is a rotor with $\Theta < 0$ deg and the minus sign if it is a stator with $\Theta > 0$ deg.

The unsteadiness as a result of blade row interactions is attributed to both the vortical wakes and the potential fields generated by the airfoils in the adjacent blade rows. With S_{exc} the tangential spacing of the airfoil row that generates the forcing function, the forcing function frequency is $\omega = 2\pi(U_w/S_{\text{exc}})$. The reduced frequency of the responding axial-flow blade row is

$$k_A = \frac{\omega C}{W_\infty} = 2\pi \frac{\cos \Theta}{\phi} \frac{C}{S} \frac{N_{\text{exc}}}{N}$$

where ϕ is the flow coefficient defined as the ratio of the through flow velocity to the rotor wheel speed based on cascade inlet conditions.

The unsteady aerodynamic blade loading is modeled by replacing each airfoil and its wake in the cascade with an unsteady vorticity distribution, with Kelvin's circulation theorem used to relate the free vorticity in the wake to the bound vorticity on the blade surface. The solution for the bound vorticity is then built up from the fundamental unsteady pressure and vorticity wave solutions, resulting in a singular integral equation

$$-\bar{w}(x_0) = \frac{1}{C} \int_0^C \gamma(x) K\left(\frac{x_0 - x}{C}\right) dx \tag{8}$$

where $\bar{w}(x_0)$ is the complex amplitude of the unsteady upwash velocity, $\gamma(x)$ is the unknown bound vorticity distribution, and $K[(x_0 - x)/C]$ is a Kernel function.[6,7]

Once the upwash velocity field is specified, the unsteady bound vorticity distribution is determined by collocation and matrix inversion subject to the Kutta condition at the trailing edge. The unsteady pressure difference across the airfoil is then determined from this vorticity distribution using the momentum equation [Eq. (2)] and given by the following expression:

$$\Delta\bar{p} = \rho_\infty W_\infty \gamma \tag{9}$$

where $\Delta\bar{p} = \bar{p}_+ - \bar{p}_-$, with the plus and minus signs referring to the upper and lower surfaces. The unsteady lift and moment acting on the blading are then calculated from this by integration.

Radial Cascade Unsteady Analysis

To predict the unsteady loading on a radial-flow turbomachine blade row due to its unsteady interaction with an adjacent airfoil row, the linear theory model considers a two-dimensional incompressible inviscid isentropic irrotational flowfield. The unsteady flow is assumed to be a small perturbation to a circumferentially uniform mean flow, with this flow described by the Laplace equation

$$\nabla^2 \Phi = 0 \tag{10}$$

Complex variable theory specifies that any function Φ of an ordered pair of real numbers x and y can be expressed solely in terms of the complex variable $z = x + iy$. Also, an analytic function $F = \Phi + i\Psi$ of the complex variable z can be defined such that Φ and Ψ are harmonic conjugates of one another that each satisfy the Laplace equation independently. Thus, every harmonic function of x and y transforms into an harmonic function of ζ and η under the change of variables $\xi + i\eta = f(x + iy)$, where f is an analytic function. If the function f is both analytic and invertible, then the transformation is termed conformal. Thus, if a potential-flow solution to the Laplace equation can be found in one domain, the solution in any other domain can be found by applying an appropriate conformal transformation.

The steady potential flow streamlines in an incompressible circumferentially uniform two-dimensional radial flow follow logarithmic spirals described by

$$\ell n(r/r_0) = \theta/\tan \alpha_L \tag{11}$$

where α_L is the angle between the streamline and a radial line, i.e., α_L is the logarithmic spiral angle and r_0 is a reference radius.

The flow through the radial cascade is transformed into that through an equivalent two-dimensional axial cascade (Fig. 2)

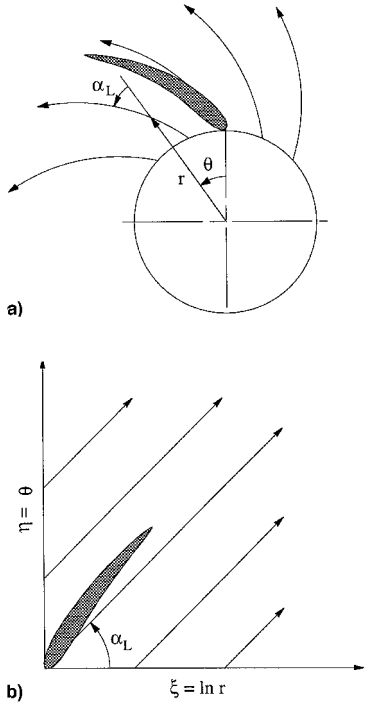

Fig. 2 Radial cascade conformal transformation: a) z and b) ζ planes.

by the following transformation that maintains the Kutta condition through the transformation of the unsteady flowfield:

$$\zeta = r_0(\ell n\, z - \ell n\, r_0) \tag{12}$$

where $\zeta = \xi + i\eta$, $z = x + iy$, and r_0 is the radius of the radial cascade exit. With this transformation the complex velocities in the two domains are related by the following expression:

$$(W_r - iW_\theta) = (r_0/r)(W_\xi - iW_\eta) \tag{13}$$

The unsteady pressure difference across an airfoil in either the axial or radial cascade can be determined using the unsteady Bernoulli equation. The value of the scalar perturbation potential Φ in the transformed axial cascade is the same as its image point in the radial cascade. However, to obtain the unsteady pressure difference across an airfoil in the radial cascade, the velocities must be multiplied by the metric of the transformation (r_0/r). The unsteady pressure difference across an airfoil in the radial cascade is thus related to the unsteady bound and free vorticity distributions in the transformed axial cascade by

$$\Delta\bar{p}_R = \rho_\infty W_\infty \left(1 - \frac{\Delta r}{r_0}\right)\left[\left(\frac{r_0}{r}\right)^2 (\gamma_A + \varepsilon_A) - \varepsilon_A\right] \tag{14}$$

where the subscripts R and A refer to the radial and transformed axial cascades, respectively, with W_∞ referenced to the airfoil leading edge in the radial cascade.

The conformal transformation of Eq. (12) maps the boundary-value problem in the radial cascade into that of an equivalent transformed axial cascade. This allows existing solution techniques developed for axial cascades to be used to obtain a solution in the transformed domain. The unsteady pressure difference across an airfoil in the radial cascade is calculated from this solution using Eq. (14), with the resulting unsteady lift and moment acting on the blading calculated from this by integration. In the axial-flow blade row analysis the cascade geometry is specified directly. However, for the radial-flow blade row analysis the radial geometry is specified and an equivalent axial cascade is calculated from the transformation defined in Eq. (12). Existing axial cascade solution techniques are then used to solve the boundary-value problem in the transformed domain. Figure 3 shows the transformation of the radial cascade into a corresponding flat-plate axial cascade.

For an incompressible axial cascade, the parameters necessary to completely specify the boundary-value problem are the solidity C/S, the stagger angle Θ, the elastic axis location x_{ea}, the reduced frequency $k_A = \omega C/W_\infty$, and σ. The parameters defining the radial cascade are the number of airfoils N, the stagger or logarithmic spiral angle α_L, the elastic axis location r_{ea}, the airfoil radial extent divided by the trailing-edge radius $\Delta r/r_0$, the reduced frequency based on the airfoil leading edge velocity k_R, and σ.

For a specified set of radial cascade parameters the corresponding axial cascade parameters can be calculated from the transformation defined in Eq. (12). The chord length, solidity, and reduced frequency in the transformed axial cascade are

$$C_A = \frac{-r_0\, \ell n(1 - \Delta r/r_0)}{\cos\alpha_L} \tag{15a}$$

$$\left(\frac{C}{S}\right)_A = -\frac{N}{2\pi}\left[\frac{\ell n(1 - \Delta r/r_0)}{\cos\alpha_L}\right] \tag{15b}$$

$$k_A = -k_R \frac{\ell n(1 - \Delta r/r_0)}{(\Delta r/r_0)(1 - \Delta r/r_0)} \tag{15c}$$

where

$$k_R = \frac{\omega\Delta r}{W_\infty \cos\alpha_L} = \frac{N_{exc}}{N}\frac{N}{\phi}\frac{(\Delta r/r_0)}{(1 - \Delta r/r_0)}$$

and ϕ is the flow coefficient defined as the ratio of the through flow velocity to the rotor wheel speed, based on cascade inlet conditions.

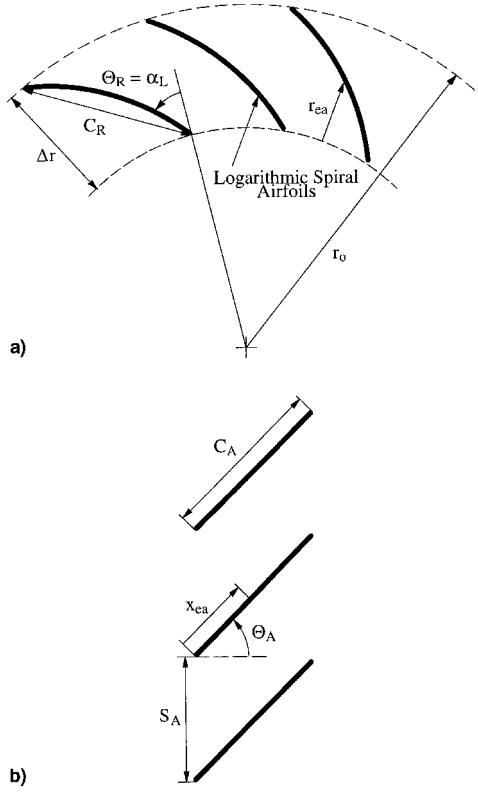

Fig. 3 Cascade transformation geometry: a) radial and b) axial cascades.

The radial spacing between the impeller exit and diffuser inlet is mapped into an equivalent axial spacing in the transformed cascade by

$$\frac{\Delta\xi}{C_A} = \frac{-\cos\alpha_L \ell n(R)}{\ell n(1 - \Delta r/r_0)} \tag{16}$$

Interaction Upwash Velocity Fields

To complete the boundary-value problems, the upwash velocity fields corresponding to the potential fields of upstream and downstream airfoil rows and the vortical wakes generated by an upstream airfoil row must be specified. The value of the scalar perturbation potential used to model the potential field of an adjacent airfoil row remains unaltered during the transformation from the axial to the radial cascade, only its functional dependence is changed. The vortical wakes shed by the impeller are described by wave solutions of the Laplace equation. Hence, in the transformed axial cascade, they are simply convected with the mean flow without decay. Thus, the specification of the upwash velocities in the transformed axial cascade completes the radial cascade boundary-value problem.

The potential field-induced upwash is derived by considering steady two-dimensional compressible uniform flow through an axial-flow blade row, described by the steady form of the perturbation velocity potential equation

$$(1 - M_\xi^2)\frac{\partial^2\Phi}{\partial\xi^2} + (1 - M_\eta^2)\frac{\partial^2\Phi}{\partial\eta^2} - 2M_\xi M_\eta \frac{\partial^2\Phi}{\partial\xi\partial\eta} = 0 \tag{17}$$

For subsonic flow this equation has solutions that are periodic in the tangential direction and decay exponentially in the axial direction

$$\Phi = \sum_{n=1}^{\infty} \bar{\Phi}_n \exp[i(k_\xi\xi + k_\eta\eta)] \tag{18}$$

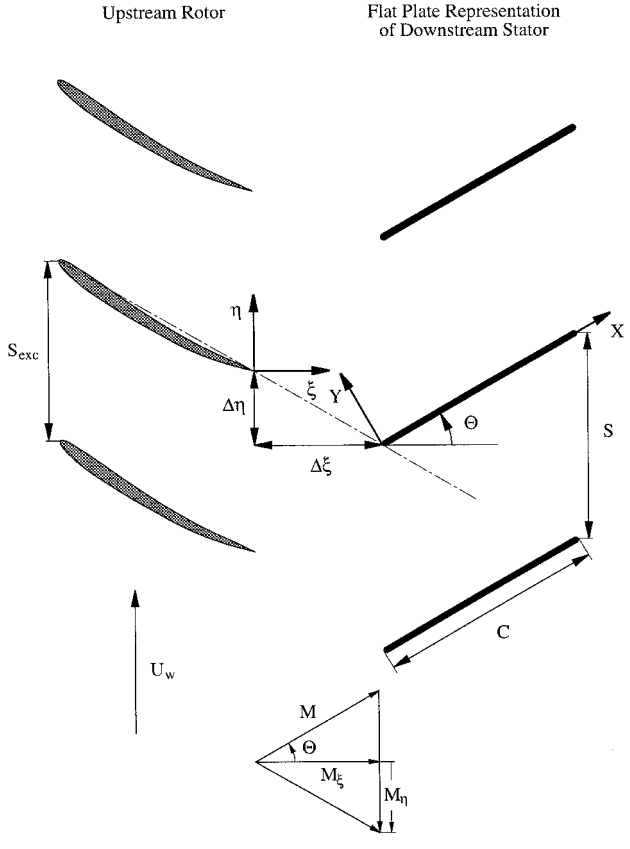

Fig. 4 Coordinate transformation to downstream stator.

where the real part of the complex expression is implied, n is the harmonic index, $\bar{\Phi}_n$ is a complex constant, $k_\eta = n(2\pi/S_{exc})$, $k_\xi = \chi k_\eta$, and

$$\chi = \frac{M_\xi M_\eta \pm \sqrt{M_\xi^2 + M_\eta^2 - 1}}{1 - M_\xi^2}$$

is a compressibility factor with the $\pm$ chosen such that $\Phi_{\pm\infty} = 0$.

As a result of the relative motion, this spatially periodic potential field induces velocities that are temporal excitations to the airfoils in the adjacent blade rows. This induced velocity field must be specified in a coordinate system attached to the adjacent airfoil row where the disturbance is unsteady. In terms of the parameters describing the responding blade row, the tangential and axial wave numbers are

$$k_\eta = \frac{\sigma}{S} \tag{19a}$$

$$k_\xi = \left[M\cos\Theta(\omega/a_\infty + k_\eta M\sin\Theta) \pm \sqrt{(\omega/a_\infty + k_\eta M\sin\Theta)^2 - (1 - M^2\cos^2\Theta)k_\eta^2}\right] /(1 - M^2\cos^2\Theta) \tag{19b}$$

To determine the effect of the potential field from an upstream airfoil row on a downstream blade row, consider a single-stage axial-flow turbomachine consisting of a rotor followed by a stator, with the stator modeled as a flat-plate airfoil cascade. At $t = 0$, the centerline of the wake shed by the upstream rotor intersects the leading edge of the reference airfoil of the downstream stator (Fig. 4). The transformation from the ξ–η coordinate system fixed to the rotor to the X–Y coordinate system attached to the responding downstream stator vane row is

$$\xi = \Delta\xi + X\cos\Theta - Y\sin\Theta \tag{20a}$$

$$\eta = \Delta\eta + X\sin\Theta + Y\cos\Theta - U_w t \tag{20b}$$

where $\Delta\xi$ is the rotor–stator axial spacing and

$$\Delta\eta = -\Delta\xi\frac{M_\eta}{M_\xi} = \Delta\xi\left(\frac{\omega/a_\infty + k_\eta M\sin\Theta}{k_\eta M\cos\Theta}\right)$$

is a phase shifting constant corresponding to the initial position at $t = 0$.

The velocity potential of the rotor blade row in a reference frame attached to the stator is obtained by substituting Eq. (20) into Eq. (18), with the velocity potential for the nth harmonic given by

$$\Phi = \bar{\Phi}_{up}\exp\{i[k_\xi(\Delta\xi + X\cos\Theta - Y\sin\Theta) + k_\eta(\Delta\eta + X\sin\Theta + Y\cos\Theta - U_w t)]\} \tag{21}$$

where $\bar{\Phi}_{up}$ is the complex amplitude of the nth harmonic of the perturbation potential at the location of the upstream rotor blade trailing edge.

The induced velocity due to the potential field of the rotor described by Eq. (21) is obtained by taking the gradient of the potential function with respect to the X–Y coordinate system, with the normal component given by $w = \partial\Phi/\partial Y$. As the responding stator vane row is modeled as a flat-plate airfoil cascade (Fig. 1), these upwash velocities must vanish at the airfoil surfaces specified by

$$X = x + mS\sin\Theta \qquad 0 \le x \le C \tag{22a}$$

$$Y = mS\cos\Theta \tag{22b}$$

where m is an index defining each airfoil's location in the cascade.

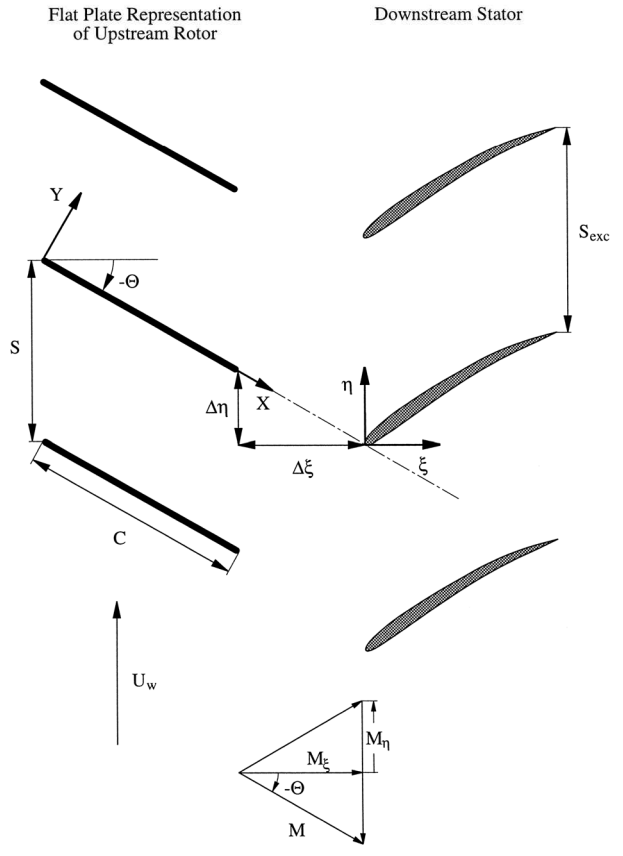

Fig. 5 Coordinate transformation to upstream rotor.

The resulting equation for the transverse component of the upwash on any airfoil in the stator cascade is

$$w = \bar{w}_{\text{up}} \exp\{i(k_\xi[\Delta\boldsymbol{\xi} + x\cos\Theta) + k_\eta(\Delta\eta + x\sin\Theta) + m\sigma + \omega t]\} \tag{23}$$

where $\bar{w}_{\text{up}}$ is the complex amplitude of the velocity normal to the stator airfoil chordline at the location of the upstream rotor blade trailing edge.

The upwash on an upstream rotor due to the potential field of a downstream stator vane row is determined in an analogous manner, with a flat-plate cascade representation of the rotor (Fig. 5). The result is

$$w = \bar{w}_{\text{dn}} \exp\big(i\{k_\xi[-\Delta\boldsymbol{\xi} + (x - C)\cos\Theta] + k_\eta[-\Delta\eta + (x - C)\sin\Theta] + m\sigma + \omega t\}\big) \tag{24}$$

where $\bar{w}_{\text{dn}}$ is the complex amplitude of the velocity normal to the rotor airfoil chordline at the location of the downstream stator vane leading edge. Note that for a multistage analysis, $\Delta\eta$ is chosen to represent the proper indexing of the upstream and downstream stators. For convenience in the present single-stage analysis, $\Delta\eta = \Delta\xi \tan\Theta$, consistent with the initial position depicted in Fig. 5.

The upwash velocity due to the wake generated by an upstream airfoil row is modeled as a simply convected vortical gust

$$w = \bar{w}_w \exp[i(-\omega/W_\infty x + m\sigma + \omega t)] \tag{25}$$

where $\bar{w}_w$ is the amplitude of the wake velocity deficit at the location of the downstream airfoil leading edge. Note that when this velocity field is transformed back to the radial cascade using Eq. (13), it corresponds to a gust that decays with the inverse of the radius.

With the potential and vortical wake upwash velocity fields specified, the unsteady pressure difference coefficients for airfoils in the axial and radial cascades can be calculated from Eqs. (9) and (14), respectively. The unsteady lift and moment coefficients are then computed by integration

$$C_{\Delta P} = \frac{\Delta\bar{p}}{\rho_\infty W_\infty^2(\bar{w}_{\text{up}}/W_\infty)}, \quad \frac{\Delta\bar{p}}{\rho_\infty W_\infty^2(\bar{w}_{\text{dn}}/W_\infty)}, \quad \frac{\Delta\bar{p}}{\rho_\infty W_\infty^2(\bar{w}_w/W_\infty)} \tag{26a}$$

$$C_L = \frac{\text{Lift}}{\rho_\infty W_\infty^2 C(\bar{w}_{\text{up}}/W_\infty)}, \quad \frac{\text{Lift}}{\rho_\infty W_\infty^2 C(\bar{w}_{\text{dn}}/W_\infty)}, \quad \frac{\text{Lift}}{\rho_\infty W_\infty^2 C(\bar{w}_w/W_\infty)} \tag{26b}$$

$$C_M = \frac{\text{Moment}}{\rho_\infty W_\infty^2 C^2(\bar{w}_{\text{up}}/W_\infty)}, \quad \frac{\text{Moment}}{\rho_\infty W_\infty^2 C^2(\bar{w}_{\text{dn}}/W_\infty)}, \quad \frac{\text{Moment}}{\rho_\infty W_\infty^2 C^2(\bar{w}_w/W_\infty)} \tag{26c}$$

where W_∞ is the velocity at the airfoil leading edge in the radial cascade.

Results

The model is utilized to demonstrate the forced response characteristics of a blade row to both potential and vortical wake forcing functions, including the differences between the response of axial- and radial-flow turbomachinery blading and the effect of Mach number. This is accomplished by analyzing the unsteady aerodynamic response of corresponding axial- and radial-flow blade rows to both potential field and vortical wake forcing functions. In this study, the responding blade row geometry is maintained constant. The number of airfoils in the adjacent blade row is varied, thereby varying both the interblade phase angle and the reduced frequency. Thus, this study provides some insight into the effect on forced response of changing the blade count ratio of a stage.

The baseline axial-flow stage, i.e., a rotor–stator, operating with a flow coefficient of 0.5 is considered. The responding axial-flow blade row of interest has a solidity of 1.5, a stagger angle of -45 deg if the rotor response to the potential field of the downstream stator is of interest, and a stagger angle of $+45$ deg when the stator response to the potential field of an upstream rotor is being analyzed. The rotor–stator axial spacing is constant, equal to 10% of the chord of the responding blade row airfoils.

The corresponding responding radial-flow blade row has 20 airfoils, $\Delta r/r_0 = 0.25$, and the same stagger angle as that of the baseline axial-flow blade row. These radial cascade parameters are chosen so that the solidity of the radial cascade based on the inlet pitch is equal to that of the corresponding responding axial cascade. The diffuser inlet to impeller exit radius ratio is 1.04, chosen so that the equivalent rotor–stator axial spacing in the transformed cascade is the same as that used for the axial-flow blade row analysis.

The response of the upstream axial-flow rotor and radial-flow impeller blades to the potential fields of the downstream stator or diffuser vane rows as a function of the blade count ratio, i.e., the interblade phase angle, are presented in Figs. 6 and 7, with the cascade inlet Mach number as a parameter. Note that the radial cascade transformation was derived for incompressible flow, with the results for nonzero Mach numbers thus only being approximate. However, these results provide insight into the effect of compressibility for radial-flow turbomachine blade rows.

For the axial-flow rotor blade row, both the amplitude and the phase angle of the unsteady lift are in good agreement with those of the incompressible analysis at the low Mach number. However, at the higher Mach number, both the amplitude and phase angle differ markedly from those of the incompressible

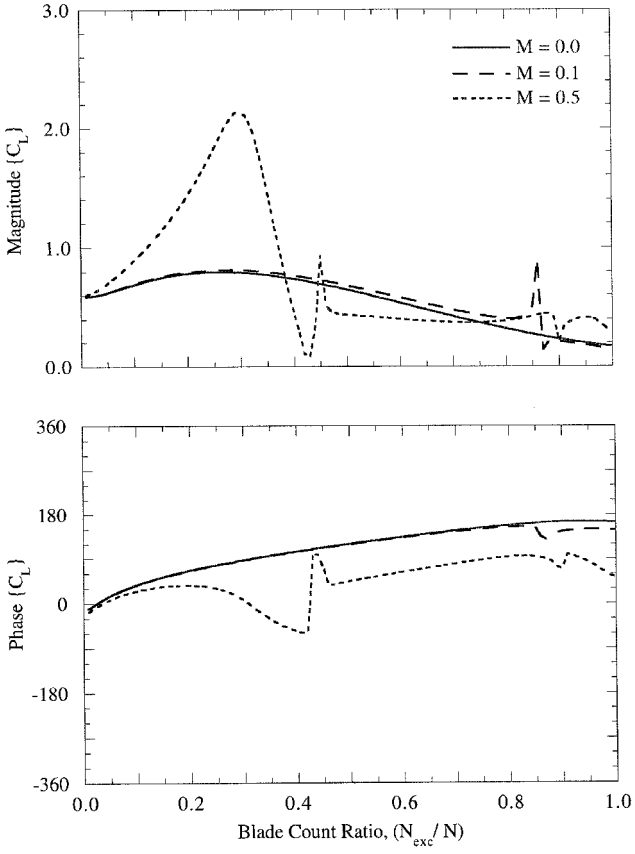

Fig. 6 Axial-flow blade row response to the downstream vane row potential field.

analysis. The discrepancies are largest when the blade count ratio is less than 0.4, with the amplitude of the unsteady lift up to $2\frac{1}{2}$ times larger and the phase angle lagging that of the incompressible analysis by as much as 180 deg. When the blade count ratio is greater than 0.45, the amplitude of the high-Mach-number response remains fairly flat, with the phase angle lagging that of the incompressible analysis by a nearly constant value of 90 deg. Note that the spikes at blade count ratios near 0.45 and 0.85 correspond to acoustic resonances that occur when the argument under the radical in Eq. (6) is zero.

For the corresponding radial-flow impeller blade row at the higher Mach number, the results are markedly different from either those of the incompressible analysis or the behavior of the axial-flow blade row at the same Mach number. The amplitude of the response remains fairly flat across the entire range of blade count ratios, in contrast to the axial-flow results that exhibited a distinct peak around a blade count ratio of 0.3. The variation in phase angle with blade count ratio is similar to that of the incompressible analysis, but with a phase lag of nearly 180 deg. At incompressible and low Mach numbers, a comparison of the predictions for the radial- and axial-flow blade rows reveals that the response amplitudes are similar, with the radial-flow blade row response being slightly larger. The variations in phase angle with blade count ratio are also similar in trend.

The downstream airfoil row, i.e., the stator in an axial-flow rotor–stator stage or the diffuser in a radial-flow impeller–diffuser stage, is subject to two forcing functions: 1) the potential field of the upstream blade row and 2) the vortical wakes shed by the upstream airfoils.

Figures 8 and 9 show the downstream axial-flow stator and radial-flow diffuser vane responses to the potential field of the upstream rotor or impeller blade row as a function of the blade count ratio, i.e., the interblade phase angle, with the cascade

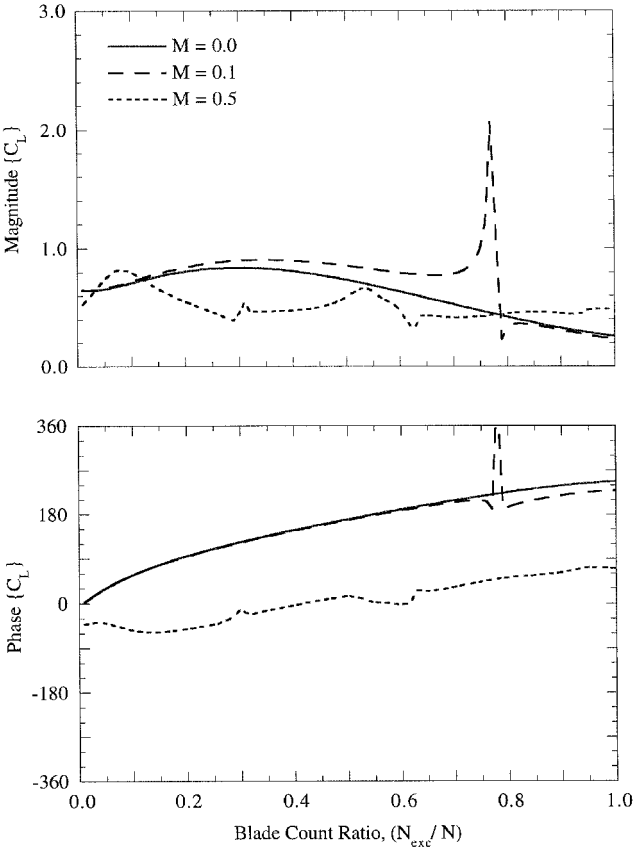

Fig. 7 Radial-flow blade row response to the downstream vane row potential field.

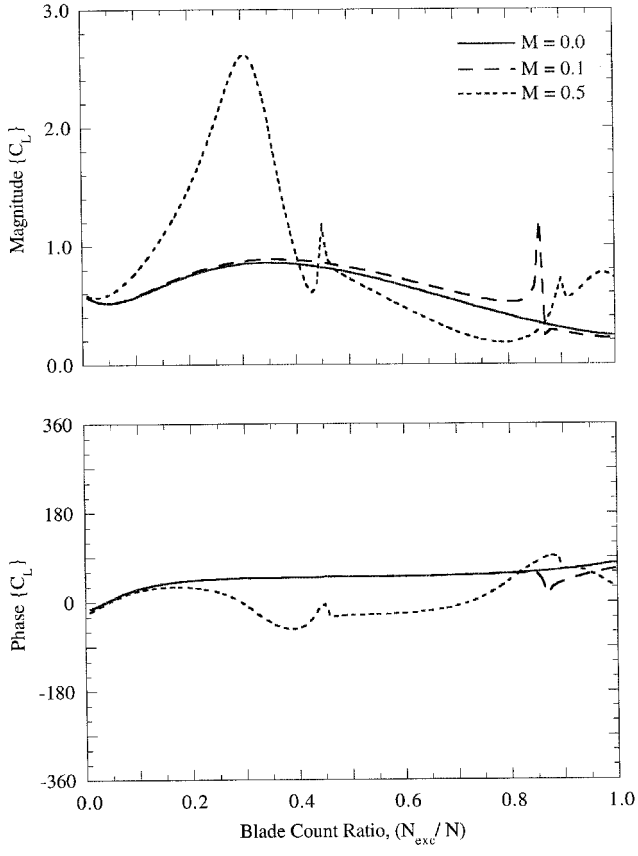

Fig. 8 Axial-flow vane row response to the upstream blade row potential field.

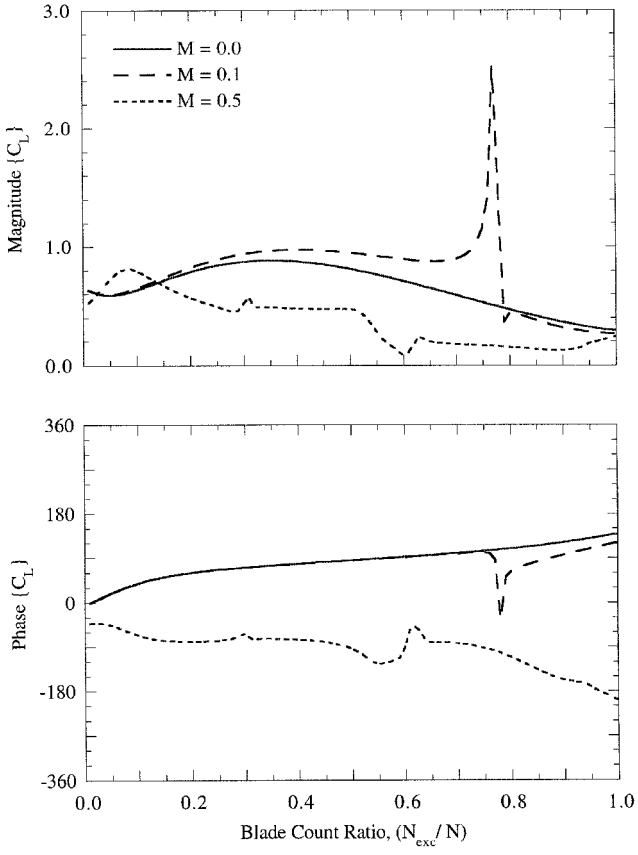

Fig. 9 Radial-flow vane row response to the upstream blade row potential field.

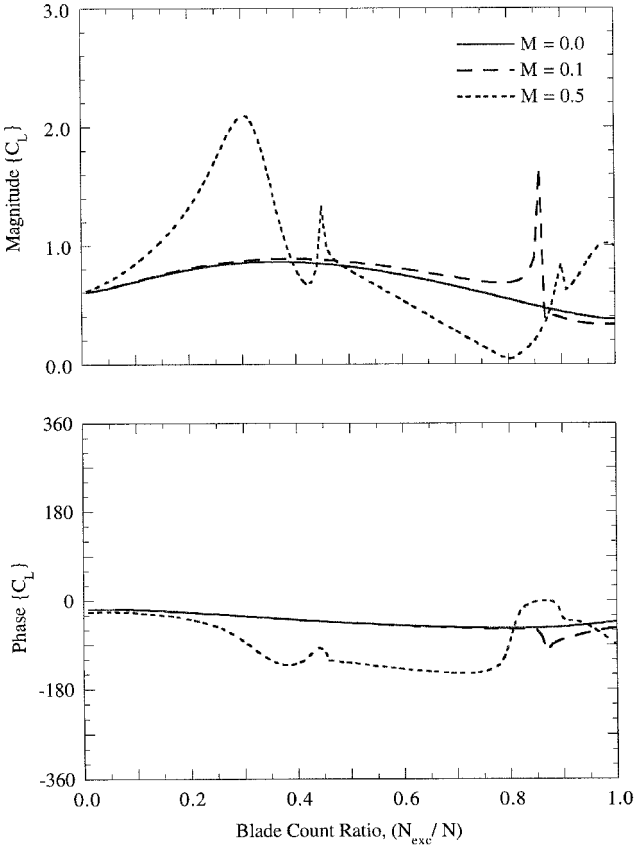

Fig. 10 Axial-flow vane row response to an upstream vortical wake.

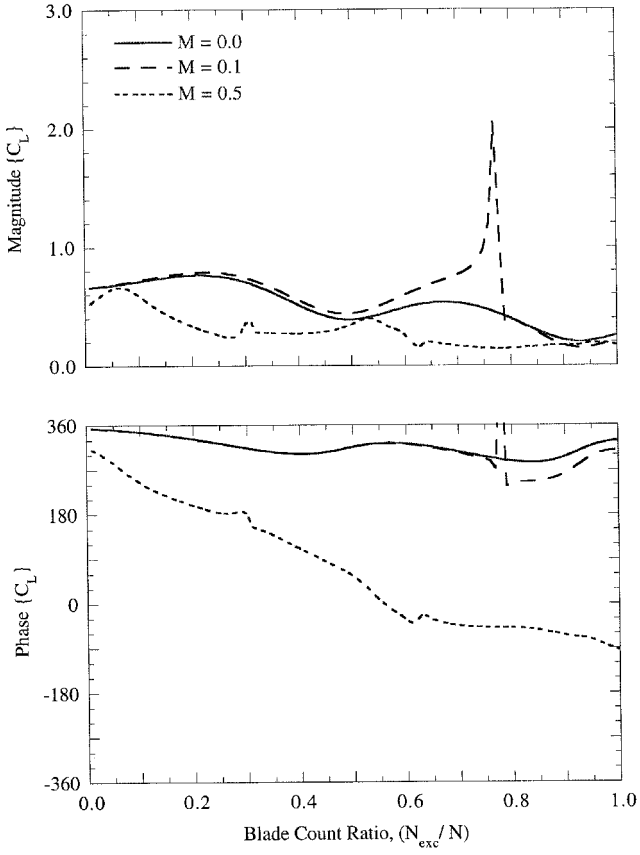

Fig. 11 Radial-flow vane row response to an upstream vortical wake.

inlet Mach number as a parameter. Both show analogous trends previously noted for the response of the upstream blade row to the potential field of a downstream airfoil row (Figs. 6 and 7). Also, for given geometry, i.e., axial or radial, the response magnitudes resulting from the upstream and downstream airfoil row potential fields are quite similar at the low Mach number, but the phase curves exhibit different trends. In particular, the response from the upstream potential field lags the response from the downstream potential field by as much as 100 deg for blade count ratios near unity. However, this behavior is dependent upon both the blade row geometry as well as the initial position of the two blade rows relative to one another, which for the present single-stage analysis was arbitrarily chosen as depicted in Figs. 4 and 5. When analyzing the response of an embedded blade row in a multistage machine, consideration must be given to the initial positions of the airfoils in the adjacent blade rows relative to one another to properly account for such phasing effects.

Figures 10 and 11 show the response of the downstream axial-flow stator and radial-flow diffuser vane responses to a simply convected vortical wake shed by the upstream blade row. For both the axial- and the radial-flow airfoil rows, the nondimensional unsteady aerodynamic response amplitudes are of the same order of magnitude as those resulting from potential field interactions (Figs. 6–9). Thus, for closely spaced, highly loaded blade rows, both wake and potential field interactions may be of equal significance. The response amplitudes of the axial-flow blade row show the same trends as those resulting from the upstream rotor potential field, but with the phase angles lagging by nearly 90 deg. For the radial-flow blade row the low-Mach-number wake response amplitudes follow a different trend than the corresponding responses from the upstream potential field. For a blade count ratio of 0.5, a minimum in the wake response occurs, at which point the response is nearly half of that caused by the upstream potential field. However, at higher Mach numbers the amplitude of the

wake response is similar to that from the upstream potential field. The phase angle of the wake response for the low-Mach-number flows is nearly 180 deg out of phase with those from the upstream potential field.

Summary and Conclusions

An unsteady aerodynamic model has been developed to predict the response of both axial- and radial-flow turbomachinery blading due to potential field interactions. For axial-flow turbomachines, this was accomplished by extending a compressible flat-plate cascade analysis to account for the induced velocities due to an adjacent blade row's potential field. The blading response in a radial cascade of logarithmic spiral airfoils was then calculated utilizing a conformal transformation mapping of the radial cascade to an equivalent axial cascade, thereby enabling existing axial cascade models to be used for radial-flow turbomachine blade rows.

The model was utilized to demonstrate the differences in the forced response of axial- and radial-flow turbomachinery blade rows resulting from both potential field and wake interactions. For both the axial- and the radial-flow blade rows, the nondimensional unsteady aerodynamic response amplitudes generated by airfoil row potential and vortical wake-forcing functions were of the same order of magnitude. Thus, for closely spaced, highly loaded blade rows, both wake and potential field interactions may be of equal significance. Also, compressibility had a profound influence on the axial-flow blade row response for high-Mach-number flows, with significant reductions in the amplitude of the unsteady lift shown to be associated with changing the blade count ratio for the stage. For low-Mach-number flows, the blading response was not as strongly affected by this change, with the axial- and radial-flow turbomachinery blade rows exhibiting similar behavior. The influence of compressibility on the radial-flow blade row response was also examined and found to not have a strong influence for the particular geometry analyzed. Finally, the unsteady lift and moment coefficients obtained with this model could be used in a first-order design system to determine the forced response behavior of the turbomachine. For an axial-flow blade row, the velocity perturbations due to the potential fields can be determined and Fourier decomposed into their harmonics using any steady potential flow-based cascade solver. For a radial-flow blade row, the potential field-induced velocity perturbations can be determined using the cascade solver in conjunction with the conformal transformation described herein.

Acknowledgment

This research was sponsored, in part, by the Army Research Office, this support is most gratefully acknowledged.

References

[1]Dring, R. P., Joslyn, H. D., Hardin, L. W., and Wagner, J. H., "Turbine Rotor-Stator Interaction," *Journal of Engineering for Gas Turbines and Power*, Vol. 104, No. 4, 1982, pp. 729–742.

[2]Smith, L. H., "Casing Boundary Layers in Multistage Axial-Flow Compressors," *Flow Research in Blading*, edited by L. S. Dzung, Elsevier, Amsterdam, 1970, pp. 275–299.

[3]Arndt, N., Acosta, A. J., Brennen, C. E., and Caughey, T. K., "Rotor-Stator Interaction in a Diffuser Pump," American Society of Mechanical Engineers, Paper 88-GT-55, New York, June 1988.

[4]Arndt, N., Acosta, A. J., Brennen, C. E., and Caughey, T. K., "Experimental Investigation of Rotor-Stator Interaction in a Centrifugal Pump with Several Vaned Diffusers," *Journal of Turbomachinery*, Vol. 112, No. 1, 1990, pp. 98–108.

[5]Kemp, N. H., and Sears, W. R., "Aerodynamic Interference Between Moving Blade Rows," *Journal of the Aeronautical Sciences*, Vol. 20, No. 9, 1953, pp. 585–597.

[6]Whitehead, D. S., "Classical Two-Dimensional Methods," *AGARD Manual on Aeroelasticity in Axial-Flow Turbomachines, Unsteady Turbomachinery Aerodynamics*, edited by M. F. Platzer and F. O. Carta, Vol. 1, AGARD-AG-298, March 1987, Chap. III.

[7]Smith, S. N., "Discrete Frequency Sound Generation in Axial Flow Turbomachines," British Aeronautical Research Council, R&M 3709, March 1972.

[8]Goldstein, M. E., and Atassi, H., "A Complete Second-order Theory for the Unsteady Flow About an Airfoil Due to a Periodic Gust," *Journal of Fluid Mechanics*, Vol. 74, Pt. 4, 1976, pp. 741–765.

[9]Hall, K. C., and Verdon, J. M., "Gust Response Analysis for Cascades Operating in Nonuniform Mean Flows," *AIAA Journal*, Vol. 29, No. 9, 1991, pp. 1463–1471.

[10]Fang, J., "Compressible Flows with Vortical Disturbances Around Cascades of Airfoils," Ph.D. Dissertation, Univ. of Notre Dame, Notre Dame, IN, April 1991.

[11]Chiang, H. D., and Turner, M. G., "Compressor Blade Forced Response Due to Downstream Vane-Strut Potential Interaction," American Society of Mechanical Engineers, Paper 93-GT-287, New York, May 1993.

[12]Simpson, H. C., Clark, T. A., and Weir, G. A., "A Theoretical Investigation of Hydraulic Noise in Pumps," *Journal of Sound and Vibration*, Vol. 5, No. 3, 1967, pp. 456–488.

[13]Bryan, W. B., and Fleeter, S., "Flow Induced Forced Response of an Incompressible Radial Cascade Including Profile and Incidence Effects," AIAA Paper 90-2352, July 1990.